Two-Dimensional Attenuated Total Reflection/Infrared Correlation Spectroscopy of Adsorption-Induced and Concentration-Dependent Spectral Variations of β-Lactoglobulin in Aqueous Solutions

Bogusława Czarnik-Matusewicz,[†] Koichi Murayama,[‡] Yuqing Wu,[§] and Yukihiro Ozaki*

Department of Chemistry, School of Science, Kwansei-Gakuin University, Uegahara, Nishinomiya 662-8501, Japan

Received: March 1, 2000; In Final Form: May 24, 2000

This paper demonstrates the potential of generalized two-dimensional (2D) attenuated total reflection/infrared (ATR/IR) spectroscopy in studies of spectral variations in the amide I region of aqueous solutions of protein. Two examples of the 2D correlation analysis are discussed in this paper. The first is concerned with adsorption-dependent spectral changes of β-lactoglobulin (BLG) in solution. The second approach is dedicated to the concentration-dependent spectral changes. To generate the 2D correlation spectra, the original spectra have been subjected to pretreatment procedures consisting of ATR correction, subtraction of the spectrum of the buffer solution, smoothing, and normalization over the concentration. The adsorption-dependent 2D study shows that the interaction between the crystal surface and the protein molecules can be monitored successfully by the synchronous and asynchronous correlation spectra. This interaction is characterized by pronounced intensity changes at frequencies assigned to β-sheet elements buried in the hydrophobic core of the molecule. The concentration-dependent 2D correlation maps, which develop 10 times more intense features than the adsorption-dependent 2D maps, are concerned with changes in various secondary structure elements located in the hydrophilic parts facing the solvent. The present study has also aimed at expanding generalized 2D correlation spectroscopy to quantitative utilization. The quantitative analysis of the 2D maps reveals that the intensity changes observed for the series of aqueous solutions of BLG with different concentrations are predominantly composed of concentration-induced secondary structure changes even in the presence of the adsorption of protein molecules to the ATR crystal.

Introduction

Despite the apparent ease and rapidity of measuring FTIR spectra of protein aqueous solutions, the analysis of the spectra is not straightforward and presents many problems. FTIR spectroscopy combined with some computational methods for resolution enhancement in amide bands has been pointed out as a powerful technique in secondary structure analysis. The earliest such methods proposed were second-derivative (SD) and Fourier self-deconvolution (FSD).[1,2] Important comments on drawbacks of these methods in secondary structure determination were addressed by Goormaghtigh et al.[3] and Mantsch et al.[4−6] More recently, some research was directed toward statistical methods[7−9] and new deconvolution procedure[10] in secondary structure studies. The major improvement over previous methods has been achieved by introducing generalized 2D correlation spectroscopy to the studies.[11−20] In addition to the capability for resolution enhancement, 2D correlation spectroscopy has another notable advantage over other techniques: it allows us to probe the specific order of the spectral intensity changes.[21]

The aim of the present study is to show the usefulness of the 2D correlation analysis in unravelling adsorption-induced and concentration-dependent ATR/IR spectral variations of β-lactoglobulin (BLG) in aqueous solutions. BLG is main component of whey proteins contained in bovine milk (more than 50 wt % of total whey proteins).[22] BLG was one of the first proteins examined by X-ray crystallographic analysis.[23] In the literature, many reported findings suggest that the secondary structure of BLG should be very sensitive to changes in its environment. Qi et al.[24] showed that the process of thermal denaturation strongly depends on the concentration of BLG, particularly in a concentration range below 50 mg/mL. Recently, Verheul et al.[25] studied the association behavior of BLG by small-angle neutron scattering. They reported that the size of the association depends on the protein concentration, pH, temperature, and ionic strength. Fox[26] collected a variety of data that show that a number of chemical and physical conditions affect the stability of BLG dimer during the denaturation process.

Perturbation-dependent structural changes in BLG have also been studied by a number of techniques, including 2D infrared (IR) and near-IR (NIR) correlation spectroscopy.[11,19] The 2D correlation studies have added greater confidence to the understanding of the changes in the conformation of BLG under various physicochemical conditions. For the external perturbation, one can select any kind of perturbation that causes the IR spectrum of the analyzed system to vary.[21,27,28] There are a

* Author to whom all correspondence should be addressed. Mailing address: Yukihiro Ozaki, Department of Chemistry, School of Science, Kwansei Gakuin University, Uegahara, Nishinomiya 662-8501, Japan. Fax: +81-798-51-0914. E-mail: ozaki@kwansei.ac.jp.

[†] Present address: Faculty of Chemistry, University of Wrocław, F. Joliot-Curie 14, 50−383 Wrocław, Poland.

[‡] Present address: Department of Environment Information and Bioproduction Engineering, Faculty of Agriculture, Kobe University, Rokkodai, Nada-ku, Kobe 657-8501, Japan.

[§] Present address: Key Laboratory of Supramolecular Structure and Spectroscopy, Jilin University, Changchun, 130023, P. R. China.

10.1021/jp0008039 CCC: $19.00
Published on Web 07/19/2000

number of papers on studies of the secondary structure of BLG under perturbations of the following conditions: temperature,[19,29−33] pH,[30,33,34] pressure,[32,33,35] hydrogen−deuterium exchange,[36] and dielectric constant of the solvent.[11,34,37] Undoubtedly, each of these perturbations induces selective intensity variations necessary for a proper 2D correlation analysis. One may wonder whether concentration can be selected as a perturbation; if each wavenumber in an IR spectrum is affected equally by a concentration variation according to the Lambert−Beer law, little new information can be obtained from a 2D correlation spectrum. This problem was examined in our previous 2D NIR study of the heat denaturation of ovalbumin, and it was revealed that concentration is also a very important perturbation for protein research.[14] Dynamic NIR spectra modulated by the concentration were utilized to construct 2D correlation spectra. However, detailed analysis of the 2D correlation spectra from the point of concentration-dependent structural changes was not carried out. The present study explores concentration-dependent structural changes in BLG. In addition, it should be noted that there is an essential difference between the current [attenuated total reflectance (ATR)/IR] and previous (NIR) experiments.[14] The former is concerned not only with the concentration-dependent changes but also with the adsorption-induced changes in the protein.

To the best of our knowledge, this is the first time that ATR/IR spectra simultaneously perturbed by adsorption processes on an ATR prism and concentration changes have ever been subjected to 2D correlation spectroscopy. Almost 10 years ago, Jakobsen and Wasacz,[38] and recently Oberg and Fink,[39] studied the influence of the protein interaction with the internal reflection element (IRE) surface on the secondary structure of the protein by use of amide bands. The presence of adsorbed and nonadsorbed (or "bulk" solution) protein molecules within the evanescent wave were detected by IR spectroscopy. Because of the interaction with the IRE, substantial structural distortions in the secondary structure of the adsorbed protein could occur. This fact cannot be neglected in the present study because the intensity values that are subjected to the 2D correlation analysis contain contributions from two kinds of perturbations, concentration changes and adsorption on the IRE surface. Both perturbations introduce significant changes in the amide bands. However, from the conventional, one-dimensional spectra, these spectral changes are not always straightforward. Therefore, in the present study, the intensity variations in the amide I band region caused by the two perturbations are explored by 2D correlation spectroscopy. In this paper, we focus our attention on the amide I band region, but in the following paper, we will report the results of the corresponding 2D correlation analysis in the amide III band region.[40] We shall also compare the 2D IR correlation analysis in the amide III region with the 2D Raman correlation analysis in the same region. Moreover, a 2D heterocorrelation analysis will be discussed in the following paper.[40]

Experimental Procedures

Bovine milk BLG was purchased from Sigma Chemical Co. and was used without further purification. Five different aqueous solutions of BLG with concentrations of 1, 2, 3, 4, and 5 wt % were prepared using a phosphate buffer at pH 6.6. To prepare water for the buffer solutions, city water was passed through activated charcoal and reverse-osmosis filters and then distilled. Finally, it was purified by an Ultrapure Water System model CPW-101 (Advantec, Japan).

The ATR/IR spectra were measured with a Nicolet Magna 760 FTIR/NIR spectrometer equipped with a liquid-nitrogen-cooled MCT detector. A total of 512 scans were co-added at a 1 cm^{-1} resolution for each spectrum. An ATR cell was made of a horizontal ZnSe crystal with an incidence angle of 45° (Spectra-Tech, Inc.). The temperature of the crystal was controlled by a thermoelectric device and kept at 25.0 ± 0.1 °C during the IR measurements. The measurement of each spectrum was started 15 min after the cell was filled with protein solution. To minimize the absorption of water vapor, the ATR equipment was purged by dry air for the duration of the measurements. After each spectral measurement, the crystal was cleaned by distilled water, and then a spectrum of the empty cell was recorded. Because protein can adsorb strongly on the crystal, we ensured that all BLG species were removed from the crystal surface before loading the next solution. To analyze the structural distortion caused by protein−crystal interactions, the cell was filled with a protein solution, and then ATR/IR spectra were obtained 15, 30, 60, 90, and 120 min after the filling. These time-dependent measurements were carried out for the 1% and 5% solutions to investigate the concentration effect on the adsorption process.

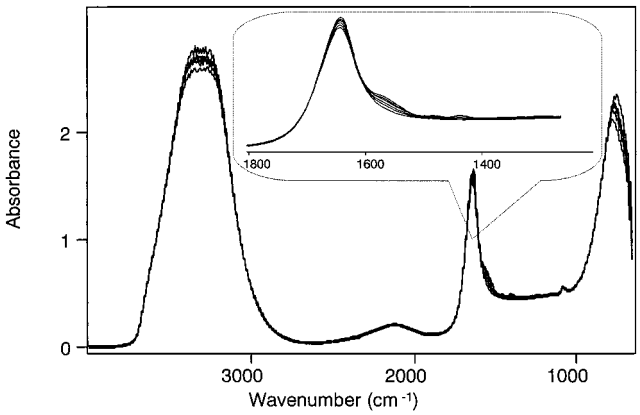

Figure 1. ATR/IR spectra in the 4000−650 cm^{-1} region of the buffer solution and five different aqueous solutions of BLG with concentrations of 1, 2, 3, 4, and 5 wt %.

Synchronous and asynchronous ATR/IR correlation spectra were calculated using the algorithm developed by Noda.[41] A subroutine named KG2D for realizing the calculation of 2D correlation spectra was composed in our laboratory using Array Basic language (GRAMS/386; Galactic Inc., Salem, NH). All data manipulation, i.e., the ATR and baseline corrections and normalization, was performed by the GRAMS program package. Spectral smoothing was achieved with the RAZOR program (Spectrum Square Associates, Inc. Ithaca, NY) also running under the GRAMS software.

Results and Discussion

Processing of the ATR spectra of BLG. Figure 1 displays the ATR/IR spectra in the 4000−650 cm^{-1} region of the buffer solution and the five different BLG solutions. As expected, the spectra are almost featureless and very close to the ATR/IR spectrum of water.

In the present study, a pretreatment procedure consisting of four steps was applied to the original spectra. As shown by Jackson and Mantsch,[42] some artifacts may be associated with the determination of the protein secondary structure by ATR/IR spectroscopy, if the dependence of the penetration depth on wavelength and refractive index is neglected. Therefore, we started the pretreatment for the ATR correction in two stages. In the first stage, each ATR spectrum was normalized over the minimum value of the penetration obtained for the analyzed

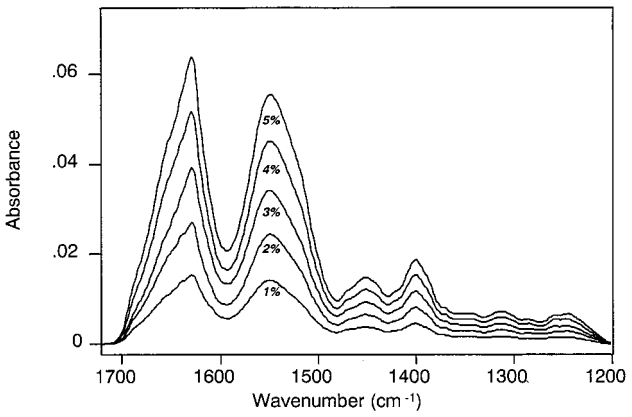

Figure 2. Concentration-dependent ATR/IR spectral variations in the 1720−1200 cm^{-1} region of the BLG solutions after the four pretreatments, except for normalization.

spectrum. The dependence of the penetration depth on the concentration was eliminated in the second stage. Finally, spectra independent of the penetration depth were obtained.

In the second pretreatment step, the contribution of water was subtracted from the spectra of the BLG solutions. Accuracy in this subtraction is crucial for obtaining reliable 2D correlation spectra.[43] Two algorithms based on a second-order least-squares fit were designed to eliminate individual bias and uncertainty in the water subtraction.[44,45] In our case, the subtraction was made using the algorithm proposed by Dosseau et al.[45] The subtracted spectra were baseline corrected by a two-point level line between 1720 and 1200 cm^{-1}. Afterward, the five subtracted spectra of BLG were smoothed by the maximum entropy method as the third pretreatment step. This method was chosen because a comparison of the Savitzky−Golay and Fourier filtering methods with the maximum entropy method showed that the latter is the most efficient in reducing the noise without distorting the band shapes.[46] Figure 2 shows the resulting spectra of the protein solutions after the four pretreatment steps.

One of the major steps in the preparation of the spectral data prior to the 2D correlation analysis is normalization. Normalization over the concentration is necessary when the concentration of the molecules studied alters simultaneously with the perturbation.[27] In principle, this should be done by dividing each one-dimensional spectrum by the corresponding concentration. However, if the exact molar concentration of the absorbing species is unknown, as in the case of the present study, the normalization should be performed in a different manner. Moreover, in the ATR experiments, the adsorption of protein on the crystal surface serves to create a locally higher concentration of protein at the solution−crystal interface than the initial concentration. In that case, values of integral intensities, calculated in the range of 1720−1200 cm^{-1}, were chosen as the normalizing factor. Thus, the normalization was the last pretreatment step before the 2D calculations for the adsorption- and concentration-dependent spectral changes were initiated.

Adsorption-Induced Structural Changes in BLG. We focus our discussion only on the amide I band in the 1700−1600 cm^{-1} region. Figure 3 shows the synchronous 2D ATR/IR spectrum generated from time-dependent spectral variations of the 5% BLG solution on the ZnSe surface. Above the 2D map, the average one-dimensional spectrum (dashed line) and power spectrum along the diagonal line of the 2D map (solid line) are presented. The power spectrum presents the overall extent of the intensity changes caused by the adsorption process. Of particular note is a comparison between the two spectra. The

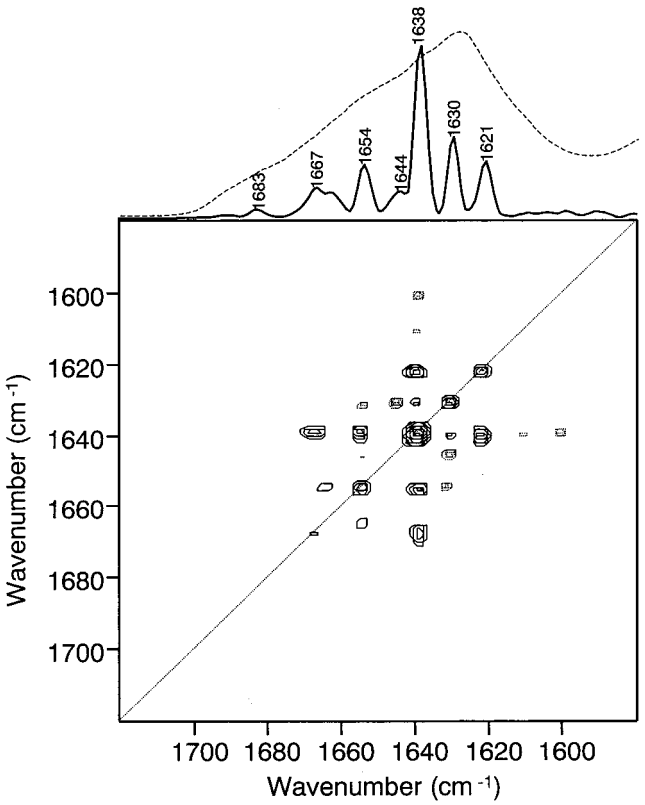

Figure 3. Synchronous 2D ATR/IR correlation spectrum in the 1720−1580 cm^{-1} region constructed from adsorption-dependent spectral changes of BLG. A power spectrum (solid line) and an averaged spectrum (dashed line) are presented at the top.

averaged spectrum can be characterized by one broad asymmetrical band with the maximum at 1628 cm^{-1} attributed to the β-sheet structure, the major structural component of BLG. In contrast, the power spectrum consists of a number of well-resolved bands barely identified in the original spectrum. In addition to the one major auto-peak observed at 1638 cm^{-1}, there are at least four auto-peaks appearing at 1667, 1654, 1630, and 1621 cm^{-1}. Positive cross-peaks, marked by solid lines, at (1667, 1638), (1654, 1638), and (1638, 1621) cm^{-1} indicate that the intensity changes correlated by these pairs of wavenumbers are either increasing or decreasing together with respect to the time-dependent adsorption process. Negative cross-peaks, marked with dashed lines at (1654, 1630) and (1644, 1630) cm^{-1}, suggest that the intensities at the higher frequencies are decreasing while the intensity at the lower frequency is increasing. In other words, at the expense of secondary structures contributing to the absorptions at 1654 and 1644 cm^{-1}, increases occur in the population of the structure associated with the absorption at 1630 cm^{-1}. The cross-peak at (1638, 1630) cm^{-1} is much less intense than the remaining cross-peaks. Therefore, the relation between the intensity changes at the two frequencies should be interpreted with caution because the sign of weak cross-peaks depends strongly on the pretreatment procedures. The absence of a cross-peak between the coordinates of 1644 and 1621 cm^{-1} suggests that the absorption variations at the two wavenumbers are uncorrelated.

The corresponding asynchronous spectrum is shown in Figure 4. Above the 2D map, a slice spectrum at 1640 cm^{-1} is given. The analysis of intensity changes in the 2D map can be simplified by extracting slice spectra. The slice spectra can provide information about the separation of overlapping bands and about the order in the intensity changes between one particular band and the others. The slice spectrum above the

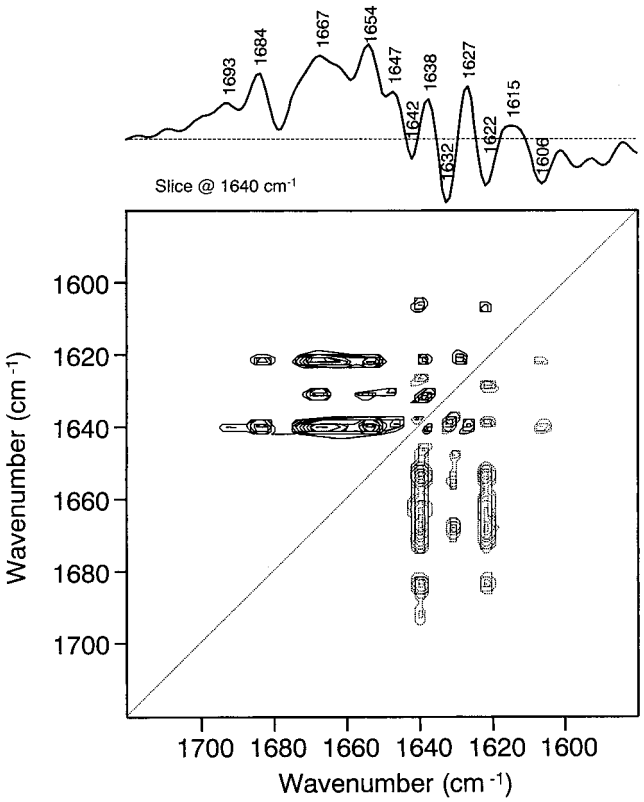

Figure 4. Asynchronous 2D ATR/IR correlation spectrum in the 1720−1580 cm^{-1} region constructed from adsorption-dependent spectral changes of BLG. A slice spectrum extracted at 1640 cm^{-1} is presented at the top.

2D map shows a number of peaks whose positions are slightly different from the positions detected by the synchronous map (Figure 3). This problem was analyzed in detail by Czarnecki,[47] Gericke et al.,[48] and Tandler et al.[49] Because asynchronous spectra are more sensitive than synchronous spectra to any intensity variations in original data, the peaks at 1693, 1627, 1615, and 1606 cm^{-1} are not identified in the corresponding synchronous spectrum shown in Figure 3.

The investigations of the adsorption- and concentration-dependent structural changes become much easier by visual inspection of the structure of BLG. Recently, a detailed X-ray crystallographic study of BLG was performed by Brownlow et al.[50] The obtained coordinates and structure factors are deposited in the Brookhaven Protein Data Bank (PDB)[51] with accession code 1BEB. A ribbon diagram of the single subunit of BLG dimer is shown in Figure 5.

Brownlow et al.,[50] in analyzing the flexibility of the dimer interface of BLG, showed that the interaction of adjacent β-sheets through the β-strands **I** is relatively more stable than the interaction between the adjacent AB loops. Moreover, Flower et al.[52] showed that these loops are more sensitive to the environment than the β-strands **A**, **F**, **G**, and **H**.

Using this PDB data, we calculated that a BLG molecule has distinct hydrophobic (53% of the backbone chain) and hydrophilic regions (47% of the backbone chain). The hydrophilic part of the backbone chain contains mainly unordered elements, whereas the hydrophobic part is dominated by the β-sheet structure. Similar calculations made for the side-chain elements show that the nonpolar amino acids are the major components of β-strands (48%). The variety of secondary structure elements shaping BLG, as well as the diversity of it electrochemical properties, makes BLG especially predisposed to planned studies.

Kinsella and Whitehead[53] analyzed the adsorption behavior of food proteins adsorbed at the air/water interface. Moreover, a variety of processes occurring at the solid/liquid interface in the presence of protein was investigated by Horbett and Brash.[54] Both groups of authors pointed out that the hydrophobic interaction is a primary factor responsible for the surface activity of proteins. On the basis of specular neutron reflectivity studies, Atkinson et al.[55] reported apparent differences in secondary structure changes between β-casein and BLG induced by the adsorption process at the air/water interface. Because the structure of β-casein is more disordered than that of BLG, much of the β-casein structure is retained. For BLG, adsorption at the interface causes the partial rearrangement of it conformations. On the basis of these studies, we infer that BLG forms at the crystal/buffer boundary a layer divided into two parts. One is more ordered, hydrophobic, and closest to the ZnSe surface, wherease the second is less ordered, hydrophilic, and extended into the bulk aqueous phase.

Because the power spectrum in Figure 3 picks up the secondary structure elements of BLG affected by the microenvironment changes due to the interaction with the crystal surface, the more intense auto-peaks below 1640 cm^{-1} can be assigned to the amide I vibrations of the β-sheet. By reference to the infrared studies of BLG in solution,[11,19,29−38,56] the peak at 1638 cm^{-1} is ascribed to a low-wavenumber component of antiparallel

Figure 5. Ribbon diagram of the single subunit of BLG, drawn from the X-ray by data Brownlow et al.[53] The diagram was produced using the program RasMol.[70]

β-strands creating the characteristic β-sheet motive "buried" in the interior of BLG. The corresponding high-wavenumber component is observed at 1693 cm^{-1}.

The band at 1630 cm^{-1} is assigned to "exposed" β-strands, i.e., those that are not part of the core of the β-sheets. The component at 1621 cm^{-1} is attributed to the formation of associated forms with a number of intermolecular hydrogen bonds. The peak at 1644 cm^{-1} is assigned to random coils, while the band at 1654 cm^{-1} represents the overlap of signals from the α-helix and random segments. The band at 1683 cm^{-1} arises mainly from the turns connecting the β-strands into the calyx. Some controversy remains in the assignment of amide I band due to 3_{10}-helices. The discrepancies concern not only BLG but also many other proteins.[57−61] On the basis of the fact that hydrogen-bond parameters of the 3_{10}-helical polypeptides are very similar to those in the β-turns but longer and less linear than those for the α-helices,[57] we assign the absorption at 1667 cm^{-1} to the 3_{10} helix structure.

The bands located below 1620 cm^{-1} are assigned to side-chain vibrations. In the BLG case, the bands could arise from tyrosine (TYR) and tryptophan (TRP) absorptions. The reactivity of individual TYR residues is essential in structural changes of BLG, e.g., in the Tanford transition.[62] The TYR and TRP residues contain important polar OH and NH groups, respectively. The native secondary structure of BLG is stabilized by the additional hydrogen bonds involving these groups. As long as the adsorption process induces structural changes, the intensity variations at the frequencies characteristic for these residues should also be observed.

In summary, the 2D synchronous map in Figure 3 reveals that the intensities attributed to the ordered β-strands buried in the hydrophobic core of BLG undergo the strongest changes in the time-dependent adsorption perturbation. The absorption changes due to the less ordered part of BLG, the part containing the β-turns and the short 3_{10}-helices of BLG, i.e., the elements most likely residing at the outer, hydrophilic surface of the protein, are almost three times less affected by the adsorption process.

According to Noda's rule for the signs of asynchronous cross-peaks,[63] we propose the following sequence of intensity changes occurring during the time-dependent adsorption process:

$$\begin{array}{c}(1693 \approx 1684 \approx \\ 1667 \approx 1654 \approx 1647) \rightarrow \\ (1640 \approx 1638) \rightarrow \\ (1632 \approx 1627) \rightarrow 1622\ cm^{-1}\end{array} \xrightarrow[\text{time of adsorption}]{}$$

According to this scheme, first to develop are changes assigned to β-turns, 3_{10}-helices, α-helices, and random coils, despite their weak intensities in the power spectrum (Figure 3). The lack of asynchronous peaks at wavenumbers assigned to these components reveals that the above secondary structures similarly respond to the adsorption-dependent perturbation. The above sequence also points out that the strongest absorption changes assigned to the buried β-strands develop before those due to the exposed β-strands, which are characterized by the less intensive power peak (Figure 3). The variations correlated with the absorptions from the intermolecularly hydrogen-bonded parts of BLG happen last among the observed changes.

Concluding, the BLG molecules become more expanded, and at the expense of the buried β-strands, increases occur in the population of the exposed β-strands, which subsequently participate in the association process. This process could also be facilitated by additional intermolecular hydrogen bonds formed between the residues located in the less ordered parts of BLG.

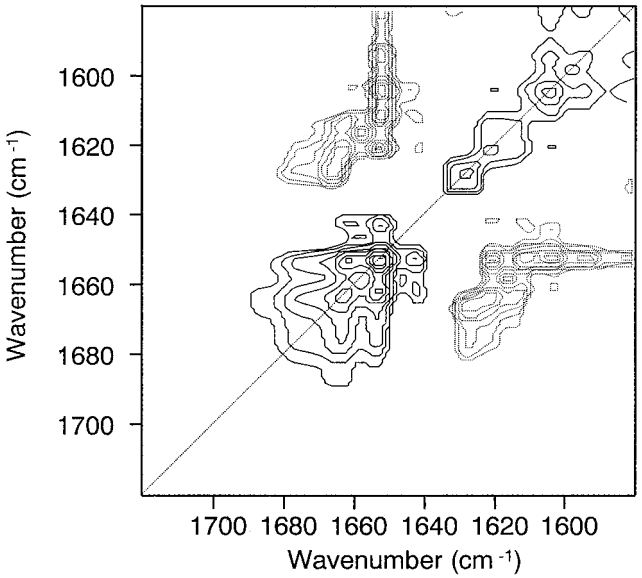

Figure 6. Synchronous 2D ATR/IR correlation spectrum in the 1720−1580 cm^{-1} region constructed from concentration-dependent spectral changes of BLG.

The interpretation of the 2D synchronous map (Figure 3) reveals that, within the evanescent wave, the populations of the exposed β-strands and the intermolecularly hydrogen-bonded parts increase with increasing time of interaction between the ATR crystal surface and the protein. At the same time, the populations of the α-helices, β-turns, and random coils decrease relatively with time. The findings reveal that partly unfolded states of BLG, which are predominantly controlled by intermolecular hydrogen bonds leading finally into larger oligomeric structures, are formed during the time-dependent adsorption.

Correct 2D correlation analysis requires normalization of the spectra over concentration. The obtained spectra for the 1% and 5% solutions were nearly identical. Consequently, the adsorption-dependent 2D maps calculated for the two concentrations matched each other. This suggests that, in BLG solutions, the adsorption process is nearly concentration-independent at least in the range of 1−5 wt %.

Concentration-Induced Structural Changes of BLG. Figure 6 depicts the synchronous 2D ATR/IR spectrum generated from the concentration-dependent spectral changes of the BLG aqueous solutions. Even at first glance, this spectrum and that in Figure 3 are quite different from each other. The discrepancies are more pronounced if the power spectra extracted from the two synchronous maps are compared with the same scale, as shown in Figure 7. The intensity changes shown by curve a are concerned solely with the adsorption process, whereas the changes presented by curve b are composed of contributions from both the adsorption process and the concentration change in the BLG solutions. It is apparent that the two curves are different from each other in terms of both quantitative and qualitative points of view.

To the best of our knowledge, except for one paper by Ekgasit and Ishida[64] presenting a general quantitative approach to 2D correlation spectra, there is no other paper devoted to the quantitative approach in 2D analysis in the literature. Generally, 2D correlation spectra can be interpreted quantitatively if the following limitations are fulfilled. First, each set of one-dimensional data for the 2D analysis must contain the same

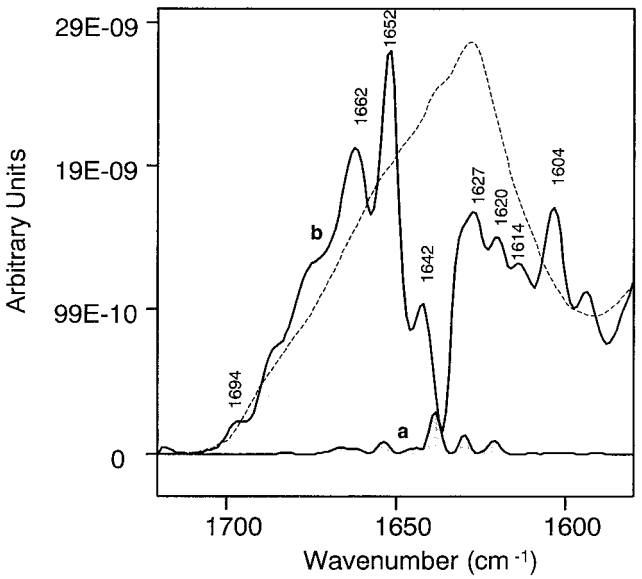

Figure 7. Power spectra along the diagonal line in the synchronous spectra constructed from the (a) adsorption- and (b) concentration-dependent spectral changes of BLG. The dashed line represents the averaged spectrum calculated from the concentration-dependent set.

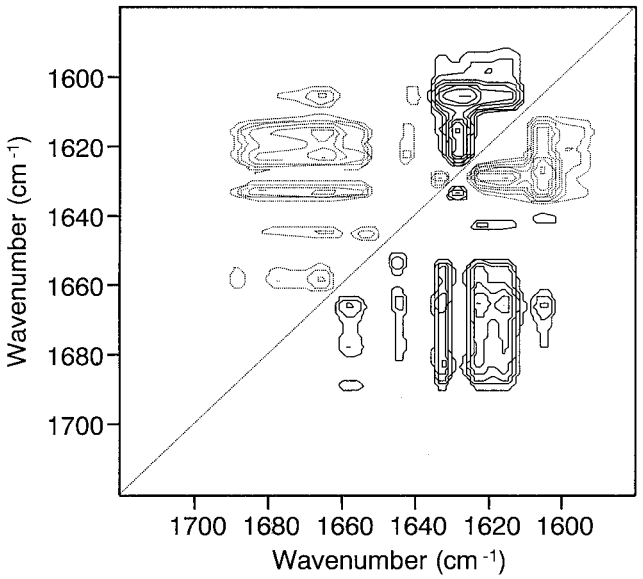

Figure 8. Asynchronous 2D ATR/IR correlation spectrum in the 1720−1580 cm^{-1} region constructed from concentration-dependent spectral changes of BLG.

number of original spectra. Second, the measured values of spectroscopic signals under some external perturbation are spread in a close range. Moreover, the choice of different reference spectra could lead to misleading quantitative conclusions. As was shown,[44] the magnitude of the dynamic spectra and the intensities of the 2D peaks depend essentially on this choice. Here, all of the presented 2D correlation spectra were calculated with respect to the perturbation-averaged spectra. In the present case, the two data sets, i.e., those perturbed by the adsorption process and those perturbed by concentration changes, comprise the above-imposed conditions. Therefore, quantitative comparison of the absorption changes induced by the two perturbations can be drawn from the 2D correlation spectra.

The analysis of the power spectra characterizing the (a) adsorption- and (b) concentration-dependent intensity changes presented in Figure 7 shows two distinct differences. First, note that the intensity variations induced only by the adsorption process are 10 times smaller than those due to the concentration and adsorption changes. Therefore, it can be concluded that the majority of intensity changes shown by curve b stem from the concentration-dependent perturbation. Thus, the influence of the adsorption process on the variations presented in Figure 7 can be neglected in the final discussion. Second, the nature of the changes represented by the two spectra is remarkably different. This fact can be interpreted as indicating that the mechanisms of secondary structure reorganization due to the two processes have different characteristics. As was shown in the previous section, the adsorption affects mainly the secondary structures buried in the hydrophobic core of the BLG molecule. On the other hand, the strongest auto-peaks detected in the power spectrum for the concentration-dependent changes (Figure 7b) appear at 1652 and 1662 cm^{-1}. These peaks are assigned to hydrophilic secondary structure elements located on the outer surface of BLG that are build from α-helices and 3_{10}-helices. These secondary structures are less protected from water penetration than the β-strands forming the calyx. The power spectrum does not contain distinct peaks assigned to turns, another highly solvent-exposed element. Only the presence of the intensive shoulder at around 1670 cm^{-1} indicates the existence of turn elements responsible for this absorption. A minimal intensity change occurs in the band at 1636 cm^{-1} assigned to antiparallel buried β-sheets. These data support the fact that the β-sheets located inside the hydrophobic core of BLG are less accessible to water molecules than those in the α-helical fragments and other hydrophilic, solvent-exposed parts of BLG. A similar conclusion was obtained by Barlow and Poole[65] on the basis of IR studies and computer-graphic analysis of high-resolution protein crystal structures.

Figure 8 shows the asynchronous correlation spectrum for the concentration-dependent spectral changes. The comparison of the asynchronous spectrum for the adsorption-dependent changes (Figure 4) with that for the concentration-dependent variations (Figure 8) reveals that the two kinds of perturbations differently affect the intensity of the amide I band. It is important to compare slice spectra extracted at the frequencies where noncorrelated intensity changes are observed individually for the adsorption- and concentration-dependent perturbations. Figure 9a and b shows such slice spectra extracted at 1640 and 1665 cm^{-1} from the asynchronous 2D spectra generated from the adsorption- (Figure 4) and concentration- (Figure 8) dependent spectral changes. The comparison between the two slice spectra shows that the unrelated intensity variations stimulated by concentration changes are at least one order of magnitude higher than those induced by the adsorption process as in the case of the power spectra. A closer inspection of the cross-peaks in the asynchronous plot (Figure 8) and the slice spectrum (Figure 9) suggests the following sequence of the spectral events occurring during the concentration increase:

$$\begin{array}{c}(1645 \approx 1642) \rightarrow \\ (1694 \approx 1683 \approx 1658 \approx 1654) \rightarrow \\ (1673 \approx 1665)\end{array} \xrightarrow{\qquad}$$

$$\begin{array}{c}(1638 \approx 1633 \approx 1628) \rightarrow \\ 1623 \rightarrow 1616 \rightarrow 1606\ cm^{-1}\end{array} \xrightarrow[\text{concentration}]{\qquad}$$

The above sequence reveals that the first event in the intensity variations is concerned with the random coil structure (1645 and 1642 cm^{-1}), followed by the intensity changes in the bands assigned to the high-wavenumber β-sheet component (1694 cm^{-1}), β-turn (1683 cm^{-1}), and α-helix (1658 and 1654 cm^{-1}). The intensity variations arising from another type of β-turn

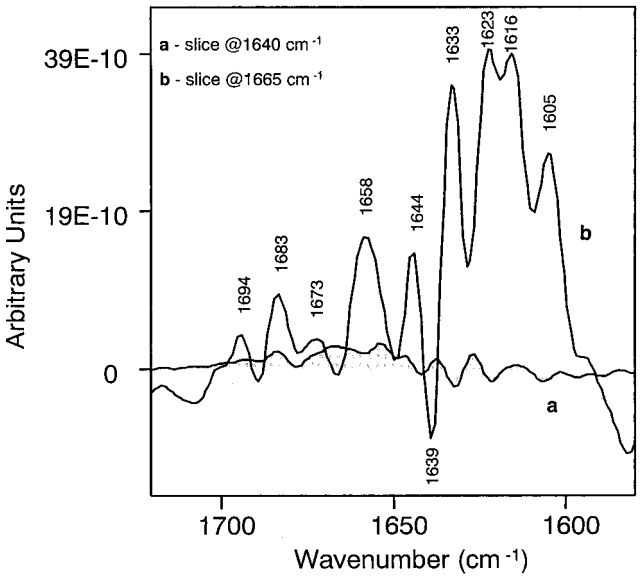

Figure 9. Slice spectra extracted along (a) 1640 cm^{-1} in the asynchronous spectrum shown in Figure 4 and (b) 1665 cm^{-1} in the asynchronous spectrum presented in Figure 8.

(1673 cm^{-1}) (probably type III) and the 3_{10}-helix (1995 cm^{-1}) occur as the next event. Meanwhile, changes attributed to both buried (1638 cm^{-1}) and exposed β-strands (1633 and 1628 cm^{-1}) occur in advance of the changes induced by associated components (1623 cm^{-1}). The last event in the sequence is attributed to the side-chain vibrations (1616 and 1605 cm^{-1}).

The minus sign of the synchronous peak around (1652, 1622) cm^{-1} suggests that, at the expense of the intramolecular hydrogen bonds located in the disordered/α-helix components, the number of intermolecular hydrogen bonds increases. This conclusion is consistent with those reached from thermal denaturation studies of BLG by infrared spectroscopy[30−33] and circular dichroism.[66] Both techniques showed that BLG does not unfold into a random coil and that a decrease in α-helix and a significant increase in β-structure in the aggregated form take place in the final stage of the thermal denaturation process.

At the moment it is very difficult to estimate how large the concentration-dependent conformational changes are. However, the present study clearly shows that the secondary structure of BLG varies significantly with concentration. It is known that most proteins do not undergo large conformational changes with concentration variation, or even upon crystallization. We plan to expand our 2D study on the concentration-dependent structural changes to other proteins to investigate whether the proteins undergo secondary structural changes with concentrations variation or not. It is also of particular interest to compare the extent of conformational changes induced by the adsorption process or the concentration changes with those created by temperature changes. Certainly, the alteration of the secondary structure of BLG induced by the heating process[30−33] is more advanced than that described in this paper. Presumably, the secondary structure of BLG is modified solely in a few percent by concentration changes and even less by the adsorption process. A quantitative and qualitative comparison of the extent of conformational changes induced by concentration and temperature changes will be reported separately.[67]

The assignments of the bands proposed in this paper are summarized in Table 1. The slight differences in the frequencies between the adsorption- and concentration-dependent changes could arise for two reasons. First, the properties of 2D correlation spectroscopy described above[49] could be responsible for the spread. Second, slight differences in the conformation between BLG adsorbed on the ZnSe surface and that in the solution are mirrored in the positions. As was revealed, the concentration changes and the adsorption process induce the structure changes. Therefore, the absorption maxima assigned to individual secondary structures detected by the two experiments may change. The synchronous spectrum does not give separate peaks corresponding to the starting and ending points of the adsorption- or concentration-dependent peak shift but yields only one value from the range detected by the asynchronous spectrum. In the examined system, as in the general cases of biological samples, we deal not only with intensity changes but also with changes in band positions and/or widths. As was discussed in detail,[48] these effects result in the appearance of additional cross-peaks in the asynchronous plot and are accompanied by errors in the peak positions of the original spectral features. An analysis of Table 1 shows that the larger discrepancies are observed for the α-helix and β-sheet components.

Finally, we will shift our attention once more to the schemes presenting the order of spectral changes taking place during the adsorption- and concentration-dependent perturbations. It can be concluded that in both perturbations, the precursors of the secondary structure changes are the random coils, turns, and α-helix elements. In contrast, the β-sheet elements are generally more resistant to adsorption- and concentration-dependent changes. Our discrimination of the two classes can be compared to a classification obtained by de Jongh et al.[68] on the basis of the H−D exchange utilized to characterization of structure and dynamics of proteins. They showed that almost all residues belonging to turns, more than 50% of residues located in random

TABLE 1: Correlation between the Secondary Structures of β-Lactoglobulin and the Amide I Frequencies Observed in the 2D Synchronous and Asynchronous Correlation Spectra and the Averaged Frequencies Calculated over the 2D Results

assignment (secondary structure)	adsorption-dependent changes		concentration-dependent changes		averaged values
	synchronous ν (cm^{-1})	asynchronous ν (cm^{-1})	synchronous ν (cm^{-1})	asynchronous ν (cm^{-1})	ν (cm^{-1})
high-wavenumber β-sheet component	−	1693	1694	1694	1694 ± 0.4
β-turn	1683	1684	−	1683, 1673	1681 ± 3.9
3_{10}-helix	1667	1667	1662	1665	1665 ± 1.8
α-helix	1654	1660, 1654	1652	1658, 1654	1655 ± 2.4
random coil	1644	1647	1642	1645, 1642	1644 ± 1.6
β-sheet buried	1638	1642, 1638	−	1639, 1636	1639 ± 1.5
β-sheet exposed	1630	1632, 1627	1627	1633, 1628	1630 ± 2.2
aggregated elements by intermolecular hydrogen bonds	1621	1622	1620	1623	1622 ± 1.0
side chains	−	1615, 1606	1614, 1604	1616, 1605	1615 ± 0.7 1605 ± 0.7

coils and those in α-helix are less protected from the exchange than β-strand residues buried inside the protein.

Conclusions

A subject of controversy in the interpretation of ATR/IR spectra of proteins, whether the major intensity variations come from the concentration changes or the adsorption process on the IRE surface, has been investigated in the present study by the use of generalized 2D correlation spectroscopy. By analyzing the spectral variations in the amide I band region induced by the adsorption and concentration perturbations, we have been able to detect distinct qualitative and quantitative differences in the spectral fluctuations caused by the two perturbations. These results demonstrate that there are two different mechanisms of secondary structure variations. In the presence of adsorption, the highly hydrophobic β-strands buried in the calyx of BLG undergo the main changes. On the other hand, the hydrophilic secondary structural elements are involved in the structural changes caused by the concentration-dependent change. The intensity variations arising from these two perturbations are examined very efficiently by comparison of the power spectra from the synchronous spectra and the slice spectra extracted at the wavenumbers of higher asynchronicity. The comparison reveals that the signal from the adsorbed layer of proteins is one order of magnitude less intense than the signal from the bulk protein. Hence, the adsorption does not affect essentially the overall band shape in amide I range. This paper has also revealed that 2D correlation spectroscopy is very sensitive technique for exploring small secondary structural changes with concentration variations. We plan to investigate the concentration-dependent structural changes of other proteins to provide a solid answer as to whether proteins undergo structural changes with concentration or not. In conclusion, the present study has opened the way for the quantitative application of generalized 2D correlation spectroscopy to the ATR/IR spectra of aqueous solutions of proteins under various conditions. In the following paper, we will extend the 2D ATR/IR study of BLG to the amide III region and attempt a 2D ATR/IR and Raman heterospectral correlation study for the same samples.

Acknowledgment. We thank Prof. Pézolet (Laval University) for his kind offer of software for the subtraction of the water spectrum. This work was supported by the Program for Promotion of Basic Research Activities for Innovative Biosciences (PROBRAIN).

References and Notes

(1) Surewicz, W. K.; Mantsch, H. H. *Biochim. Biophys. Acta* **1988**, *952*, 115.
(2) Arrondo, J. L. R.; Muga, A.; Castresana, J.; Goñi, F. M. *Prog. Biophys. Mol. Biol.* **1993**, *59*, 23.
(3) Goormaghtigh, E.; Cabiaux, V.; Ruysschaert, J. M. *Subcellular Biochemistry*; Hilderson, H. J., Ralston, G. B., Eds.; Plenum Press: New York, 1994; Vol. 23, Chapter 10.
(4) Surewicz, W. K.; Mantsch, H. H.; Chapman, D. *Biochemistry* **1993**, *32*, 389.
(5) Jackson, M.; Mantsch, H. H. *CRC Crit. Rev. Biochem. Mol. Biol.* **1995**, *30*, 1995.
(6) Jackson, M.; Mantsch, H. H. *Infrared Spectroscopy of Biomolecules*; Mantsch, H. H., Chapman, D., Eds.; John Wiley & Sons: New York, 1996; Chapter 11.
(7) Dousseau, F.; Pezolet, M. *Biochemistry* **1990**, *29*, 8771.
(8) Lee, D. C.; Haris, P. I.; Chapman, D.; Mitchell, R. C. *Biochemistry* **1990**, *29*, 9185.
(9) Wi, S.; Pancoska, P.; Keiderling, T. A. *Biospectroscopy* **1998**, *4*, 93.
(10) Bramanti, E.; Benedetti, E. *Biopolymers* **1995**, *38*, 639.
(11) Sefara, N. L.; Magtoto, N. P.; Richardson, H. H. *Appl. Spectrosc.* **1997**, *51*, 536.
(12) Nabet, A.; Pezolet, M. *Appl. Spectrosc.* **1997**, *51*, 466.
(13) Graff, D. G.; Pastrana-Rios, B.; Venyaminov, S. Y.; Prendergast, F. G. *J. Am. Chem. Soc.* **1997**, *119*, 11282.
(14) Wang, Y.; Murayama, K.; Myojo, Y.; Tsenkova, R.; Hayashi, N.; Ozaki, Y. *J. Phys. Chem.* **1998**, *102*, 11282.
(15) Schultz, C. P.; Fabian, H.; Mantsch, H. H. *Biospectroscopy* **1998**, *4*, S19.
(16) Fabian, H.; Mantsch, H. H.; Schultz, C. P. *Proc. Natl. Acad. Sci.* **1999**, *96*, 13153.
(17) Pancoska, P.; Kubelka, J.; Keiderling, T. A. *Appl. Spectrosc.* **1999**, *53*, 647.
(18) Smeller, L.; Heremans, K. *Vib. Spectrosc.* **1999**, *19*, 375.
(19) Sefara, N. L.; Green, T. K.; Richardson, H. H. *Biospectroscopy*, in press.
(20) Sonoyama, M.; Nakano, T. *Appl. Spectrosc.*, in press.
(21) Noda, I. *Appl. Spectrosc.* **1993**, *47*, 1329.
(22) Fox, P. F. *Advanced Dairy Chemistry-1: Proteins*; Elsevier: New York, 1992.
(23) Crowfoot, D. M.; Riley, D. P. *Nature* **1938**, *141*, 521.
(24) Qi, X. L.; Brownlow, S.; Holt, C.; Sellers P. *Biochim. Biophys. Acta* **1995**, *1248*, 43.
(25) Verheul, M.; Pedersen, J. S.; Roefs, S. P. F. M.; de Kruif, K. G. *Biopolymers* **1999**, *49*, 11.
(26) Fox, P. F. *Heat Induced Changes in Milk*, 2nd ed.; International Dairy Federation: Brussels, Belgium, 1995.
(27) Marcott, C.; Noda, I.; Dowrey, A. E. *Anal. Chem. Acta* **1991**, *259*, 131.
(28) Czarnecki, M. A. *Appl. Spectrosc*. **1999**, *53*, 1392.
(29) Kaiden, K.; Matsui, T.; Tanaka, S. *Appl. Spectrosc*. **1987**, *41*, 180.
(30) Casal, H. L.; Köhler, U.; Mantsch, H. H. *Biochim. Biophys. Acta* **1988**, *957*, 11.
(31) Qi, X. L.; Holt, C.; McNulty, D.; Clarke, D. T.; Brownlow, S.; Jones, G. R. *Biochem. J.* **1997**, *324*, 341.
(32) Panick, G.; Malessa, R.; Winter, R. *Biochemistry* **1999**, *38*, 6512.
(33) Allain, A. F.; Paquin, P.; Subirade, M. *Int. J. Biol. Macromol*. **1999**, *26*, 337.
(34) Dufour, E.; Robert, P.; Bertrand, D.; Haertle, T. *J. Protein Chem*. **1994**, *13*, 143.
(35) Subirade, M.; Loupil, F.; Allain, A. F.; Paquin, P. *Int. Dairy J*. **1998**, *8*, 135.
(36) Dong, A.; Matsuura, J.; Allison, S. D.; Chrisman, E.; Manning, M. C.; Carpenter, J. F. *Biochemistry* **1996**, *35*, 1450.
(37) Dong, A.; Matsuura, J.; Manning, M. C.; Carpenter, J. F. *Arch. Biochem. Biophys*. **1998**, *355*, 275.
(38) Jakobsen, R. J.; Wasacz, F. M. *Appl. Spectrosc*. **1990**, *44*, 1478.
(39) Oberg, K. A.; Fink, A. L. *Anal. Biochem*. **1998**, *256*, 92.
(40) Jung, Y. M.; Czarnik-Matusewicz, B.; Ozaki, Y. *J. Phys. Chem.* **2000**, *104*, 7812.
(41) Noda, I. *Appl. Spectrosc*., in press.
(42) Jackson, M.; Mantsch, H. H. *Appl. Spectrosc*. **1992**, *46*, 699.
(43) Czarnik-Matusewicz, B.; Czarnecki, M. A.; Ozaki, Y. In *Proceedings of the International Symposium on Two-Dimensional Correlation Spectroscopy 1999*; American Institute of Physics: Woodbury, NY, 2000; p 291.
(44) Powell, J. R.; Wasacz, F. M.; Jakobsen, R. J. *Appl. Spectrosc*. **1986**, *40*, 339.
(45) Dousseau, F.; Therrien, M.; Pezolet, M. *Appl. Spectrosc*. **1989**, *43*, 538.
(46) Echabe, I.; Encinar, J. A.; Arrondo, J. L. R. *Biospectroscopy* **1997**, *3*, 469.
(47) Czarnecki, M. A. *Appl. Spectrosc*. **1998**, *52*, 1583.
(48) Gericke, A.; Gadaleta, S. J.; Brauner, J. W.; Mendelsohn, R. *Biospectroscopy* **1996**, *2*, 341.
(49) Tandler, P. J.; Harrington, P. B.; Richardson, H. *Anal. Chim. Acta* **1998**, *368*, 45.
(50) Kinsella, J. E.; Whitehead, D. M. *Proteins at Interfaces*; Brash, J. L., Horbett, T. A., Eds.; ACS Symposium Series 343; American Chemical Society: Washington, D.C., 1987; Chapter 39.
(51) Horbett, T. A.; Brash, J. L. *Proteins at Interfaces*; Brash, J. L., Horbett, T. A., Eds.; ACS Symposium Series 343; American Chemical Society: Washington, D.C., 1987; Chapter 1.
(52) Atkins, P. J.; Dickinson, E.; Horne, D. S.; Richardson, R. M. *J. Chem. Soc., Faraday Trans*. **1995**, *91*, 2847.
(53) Brownlow, S.; Cabral, J. H. M.; Cooper, R.; Flower, D. R.; Yewdall, S. J.; Polikarpov, I.; North, A. C. T.; Sawyer, L. *Structure* **1997**, *5*, 481.
(54) Protein Data Bank, Department of Chemistry, Brookhaven National Laboratory, Upton, NY, 1973. http://www.pdb.bnl.gov/pdb/index.html.
(55) Flower, D. R.; North, A. C. T.; Attwood, T. K. *Protein Sci*. **1993**, *2*, 753.
(56) Byler, D. M.; Susi, H. *Biopolymers* **1986**, *25*, 469.

(57) Prestelski, S. J.; Byler, D. M.; Thompson, M. P. *Int. J. Peptide Protein Res.* **1991**, *37*, 508.
(58) Jackson, M.; Mantsch, H. H. *Can. J. Chem*. **1991**, *69*, 1639.
(59) Wilder, Ch. L.; Friedrich, A. D.; Potts, R. O.; Daumy, G. O.; Francoeur, M. L. *Biochemistry* **1992**, *31*, 27.
(60) Hadden, J. M.; Chapman, D.; Lee, D. C. *Biochim. Biophys. Acta* **1995**, *1248*, 115.
(61) Chehin, R.; Iloro, I.; Marcos, M. J.; Villar, E.; Shnyrov, V. L.; Arrondo, J. L. R. *Biochemistry* **1999**, *38*, 1525.
(62) Qin, B. Y.; Bewley, M. C.; Creamer, L. K.; Baker, H. M.; Baker, E. N.; Jameson, G. B. *Biochemistry* **1998**, *37*, 14014.
(63) Noda, I. *Appl. Spectrosc*. **1990**, *44*, 550.
(64) Ekgasit, S.; Ishida, H. *Appl. Spectrosc*. **1995**, *49*, 1243.
(65) Barlow, D. J.; Poole, P. L. *FEBS Lett.* **1987**, *213*, 423.
(66) Sawyer, W. H.; Norton, R. S.; Nichol, L. W.; McKenzie, G. H. *Biochim. Biophys. Acta* **1971**, *243*, 19.
(67) Czarnik-Matusewicz, B.; Ozaki, Y., manuscript in preparation.
(68) de Jongh, H. H. J.; Goormaghtigh, E.; Ruysschaert, J. M. *Biochemistry* **1997**, *36*, 13603.
(69) Sayle, R. *RasWin Molecular Graphics*, Windows version 2.6; University of Massachusetts, Amherst, MA, 1995.